

# EFFECT OF PVD PROCESS PARAMETERS ON THE TiAlN COATING ROUGHNESS

A.R Md Nizam<sup>1</sup>, P. Swanson<sup>2</sup>, M. Mohd Razali<sup>1</sup>,  
B. Esmar<sup>1</sup>, H. Abdul Hakim<sup>3</sup>

<sup>1</sup>Faculty of Manufacturing Engineering, Universiti Teknikal Malaysia Melaka, Locked Bag 1752, Pejabat Pos Durian Tunggal, 76109 Durian Tunggal, Melaka.

<sup>2</sup>Faculty of Engineering and Computing, Coventry University, Priory Street, Coventry CV1 5FB. United Kingdom.

<sup>3</sup>Advanced Materials Research Center, Sirim Berhad, No 34, Jalan Hi Tech 3/4, Kulim High Tech Park 09000 Kulim Kedah

## ABSTRACT

*Coating on cutting tools has been proven to improve tool life significantly. Physical Vapour Deposition sputtering process is one of the main techniques to deposit coating on cutting tool. One of the coating characteristics that influence its performance is coating surface roughness. Extensive research has been carried out to understand the effect of process parameters on the resulting coating roughness. However holistic study to understand the combination of parameters and their interactions are lacking. The objective of this study is to evaluate the effect of coating process parameters (substrate bias voltage, substrate temperature, and sputtering power) on the deposited TiAlN coating roughness using response surface methodology. Coating roughness characterization was done using Atomic Force Microscopy apparatus. Aside from that coating microstructure was also investigated using XRD and SEM. Finding from this research suggested that sputtering power, interaction between sputtering power and substrate temperature, and substrate bias quadratic term significantly influence the deposited coating surface roughness.*

**KEYWORDS:** *Sputtering, TiAlN, surface roughness, PVD, interaction, RSM*

## 1.0 INTRODUCTION

The application of thin film coating on cutting tools can significantly improve cutting tool performance by enhancing the surface properties of the tool. The improved performance of coated cutting tools has been proven and documented (K. Laing *et.al.*, 1999) (O. Gekonde Haron *et.al.*,

2002) (G. Byrne *et al.*, 1993) (K. Tuffy *et al.*, 2004). One particular study done by Tuffy *et al.* indicated that coated tool wear performance was forty times better than the uncoated tools (K. Tuffy *et al.*, 2004). Aside from prolonging tool life, coated tools can also enable the implementation of Minimum Quantity Lubrication (MQL) and pursuant of dry machining. This can drastically reduce manufacturing cost associated with cutting fluids, which attribute to about 15% of metal cutting manufacturing costs, and minimize environmental impact associated with disposal of cutting fluid (G. Byrne *et al.*, 1993). One of the coating characteristics that have significant influence on cutting tool performance is surface roughness of the developed coating. Surface roughness can influence the friction level and material pick-up behaviour of cutting tool upon sliding with other material (B. Podgornik *et al.*, 2004).

Two main techniques in depositing coating on cutting tool are physical vapour deposition (PVD) and chemical vapour deposition (CVD). The fundamental difference between the two processes is the vapour source. As the name indicates, the vapour source for PVD originates from a solid target from which atoms are displaced and vapour source for CVD originated from a chemical vapour precursor. In PVD process, the vaporization of the solid target may be done through heating or sputtering; this work focuses on the PVD sputtering process only. The PVD sputtering process involves the ejection of particles from target material due to the collision of highly energetic projectile particles (e.g. Argon ions) with the target surface (Bunshah *et al.*, 1994).

Coating process optimization requires good understanding of the factors that influence coating characteristics. PVD process parameters have a significant influence on the resultant coating characteristics including the coating roughness (Musil *et al.*, 1998), (Smith *et al.*, 1995), (Mayrhofer *et al.*, 2006). Some of the experimental work done on PVD process indicated that substrate bias voltage, sputter power, and substrate temperature could have significant effects the deposited coating roughness (Barshilia *et al.*, 2004), (Xu *et al.*, 2006).

The objective of this study is to investigate the effect of substrate bias voltage, substrate temperature and sputtering power on the deposited coating roughness using response surface methodology (RSM). This holistic approach in assessing the behaviour of the PVD process is lacking in the previous studies.

## 2.0 EXPERIMENT

The TiAlN coating was deposited onto the tungsten carbide (WC) cutting tool insert using an unbalanced magnetron sputtering system made by VACTEC Korea, model VTC PVD 1000. The target was Ti-Al alloy targets (50 % Ti: 50 % Al). Prior to coating, the substrates were cleaned using an ultrasonic cleaner with alcohol bath for 20 minutes. The coating process throughout the experiment consisted of three stages; in-situ substrate etching for 30 minutes, interlayer coating (TiAl of approximately 0.2 micron), and coating deposition (TiAlN). The base pressure before the initiation of coating process was set at  $5.0 \times 10^{-5}$  mbar. The deposition of TiAlN was done in the Ar and  $N_2$  partial pressure environment of  $4.0 \times 10^{-3}$  mbar and  $0.4 \times 10^{-3}$  mbar respectively for 90 minutes.

The experimental matrix and data analysis were based on the on RSM centre cubic design, using Design Expert version 7.0.3 software. It consisted of 8 factorial points, 4 axial points and 6 central points to enable an estimation of process variability as illustrated by Figure 1. The experimental matrix was designed based on assigning the extreme points (operating window) as the +/- Alpha value, refer to Table 1. Based on the defined extreme point values, the software then assigned the high and low settings for the factorial points. This was to ensure the characterization could be performed covering the widest range of operating window possible for respective parameters. Because of this the value of factorial points were not nicely rounded. The developed experimental matrix based on the RSM central composite design and the +/- Alpha values defined in Table 1, are as shown in Table 2.

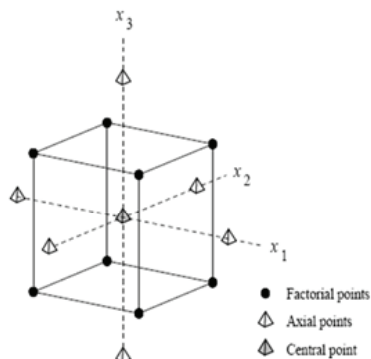


FIGURE 1  
RSM Central Composite Design for 3 factors at two levels

TABLE 1  
Extreme operating window for respective process parameters

	Substrate temperature ( °C )	Substrate bias voltage (V)	Sputter power (kW)
- Alpha	200	50	4
+ Alpha	600	300	8

## 2.1 Coating procedures

Coating roughness and microstructure analysis technique were performed following these procedures:

### 2.1.1 Atomic Force Microscopy (AFM)

The roughness of the developed TiAlN thin film coatings were analysed using Shimadzu SPM-9500J2 AFM apparatus. The detection mode used was contact mode using a commercial Si<sub>3</sub>N<sub>4</sub> cantilever and the scanning area was set at 5x5 microns (25 μm<sup>2</sup>).

### 2.1.2 X-ray Diffraction (XRD)

The XRD analyses were performed using Bruker D-8 XRD apparatus. Due to the thin film sample, a grazing incidence angle (GIA) feature was utilized with a grazing angle of 1 degree. The analysis was done using CuKα radiation with λ = 0.15406 nm with Ni filter, operated at 40 kV and 40 mA. The 2θ scanning range was set between 30 to 60 degrees with a step size of 0.020 degree and a dwell time of 1 second. The 2θ scanning range was selected to capture two main peaks appeared for the developed coating, TiAlN (111) and (200). The identification of TiAlN (111) and (200) peaks are based on standard JCPDS No: 37-1140; the peaks at 37.7° and 43.8° correspond to diffraction along 111 and 200 planes respectively. The quantitative data extracted from the XRD analysis are the I(111)/ I(200) and the grain size. The grain size (D<sub>p</sub>) data was collected on dominant XRD peak of either (111) or (200) using Scherrer's equation  $D_p = 0.9 \lambda / \beta 2\theta \cos\theta$  (Culity *et al.*, 1972); Where λ is the wavelength of the X-ray, θ is the Bragg's angle and β2θ is the FWHM of 111 or 200 peak of the XRD pattern.

### 2.1.3 Scanning Electron Microscopy (SEM)

The analyses were performed using SEM/EDX LEO-1525. SEM image captured the cross section view of fractured coating deposited on WC substrate.

### 3.0 RESULTS AND DISCUSSIONS

The twenty experimental run results are listed in Table 2. The roughness data, in nanometres (nm), for the developed coating of each experimental run is tabulated in Table 2.

TABLE 2  
Experimental run and results of coating roughness

Run	Factor 2	Factor 2	Factor 3	Response 1
	A:Sputter Power	B:Bias Voltage	C:Substrate Temperature	Roughness
	(kW)	(Volts)	(°C)	(nm)
1	6	50	400	81.00
2	4.81	100.67	518.92	65.60
3	4.81	249.33	281.08	81.90
4	6	175	400	70.30
5	6	175	200	58.80
6	4.81	100.67	281.08	75.60
7	7.19	249.33	281.08	44.30
8	6	175	400	48.10
9	6	175	400	43.70
10	4.81	249.33	518.92	56.10
11	7.19	100.67	281.08	49.90
12	6	175	600	56.00
13	7.19	249.33	518.92	49.10
14	6	175	400	57.90
15	8	175	400	40.20
16	6	300	400	100.00
17	7.19	100.67	518.92	67.30
18	4	175	400	47.40
19	6	175	400	45.00
20	6	175	400	63.60

Determination of significant factors influencing resultant coating roughness and the presence of interactions affecting the surface roughness were done by carrying out analysis of variance (ANOVA) on the experimental data. The ANOVA analysis is shown in Table 3. Based on the p-value of less than 0.1, sputtering power, interaction between sputtering power and substrate temperature, and substrate bias quadratic term are the significant influencing factors of the resultant surface roughness.

TABLE 3  
ANOVA for coating roughness model

Source	Sum of Squares	df	Mean Square	F Value	p-value Prob > F
Model	3619.45	9	402.16	3.88	0.0229
A-Sputter Power	476.97	1	476.97	4.61	0.0574
B-Bias Voltage	1.8	1	1.8	0.017	0.8978
C-Substrate Temperature	24.55	1	24.55	0.24	0.6368
AB	53.04	1	53.04	0.51	0.4905
AC	420.5	1	420.5	4.06	0.0716
BC	100.82	1	100.82	0.97	0.3471
A <sup>2</sup>	299.49	1	299.49	2.89	0.1198
B <sup>2</sup>	2058.74	1	2058.74	19.88	0.0012
C <sup>2</sup>	0.9	1	0.9	8.67E-03	0.9276
Residual	1035.53	10	103.55		
Lack of Fit	444.1	5	88.82	0.75	0.6196
Pure Error	591.43	5	118.29		
Cor Total	4654.98	19			

Discussions on the influence of sputtering power, interaction between sputtering power and substrate temperature, and substrate bias quadratic term are as the following:

### 3.1 Sputtering power:

As the sputtering power increases from 4.81kW to 7.19kW, coating roughness reduced from 56.2 nm to 44.4 nm. (Figure 2). This is aligned with findings by Wuhrer and Yeung who reported a decrease in roughness with the increase in sputtering power (Wuhrer et al., 2004).

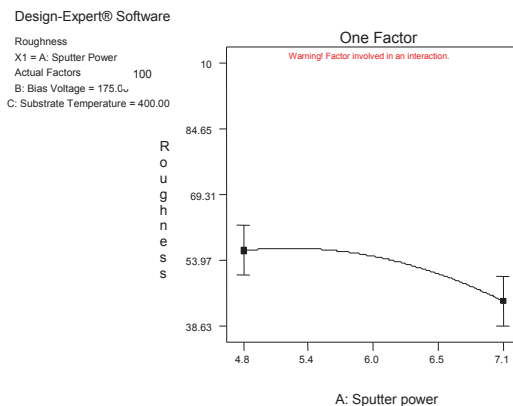


FIGURE 2  
Behaviour of coating roughness in response to variation of sputtering power

The decrease in roughness as the sputter power increases can be explained by investigating the microstructure of the developed coating. The  $2\theta$  vs. intensity XRD curves for sputter power of 4kW, 6kW and 8kW are shown in Figure 3. The quantitative data from the XRD analysis such as I111/I200 and grain size are tabulated in Table 4. The XRD curves in Figure 3 indicates the shift in dominant peak of crystal orientation from (111) to (200) as the sputter power increases from 4kW to 8 kW. This is also reflected by the peak intensity ratio of the two, I111/I200, in Table 4. The I111/I200 ratio indicates that no significant peak of (200) can be found at the low sputter power of 4 kW. However the (200) peak become dominant at the sputter power of 8 kW level. This trend was also reported by Xu et al. (Xu *et al.*, 2006) and Wuhrer and Yeung (Wuhrer *et al.*, 2004) based on their study of TiN coating and TiAlN coating deposited using the same PVD sputtering technique.

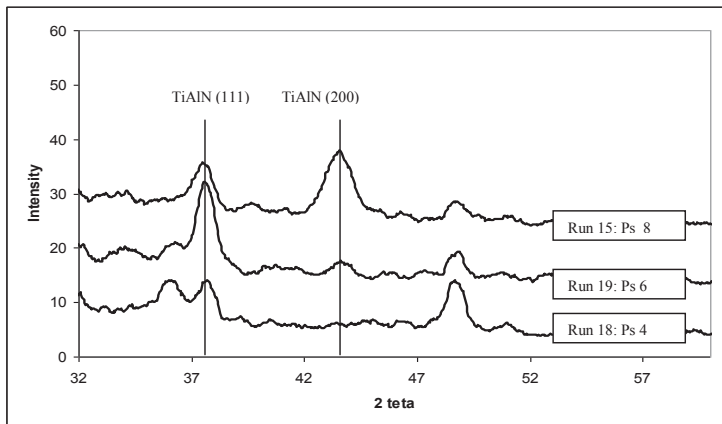


FIGURE 3

The  $2\theta$  vs intensity XRD curves for sputtering power of 4 kW, 6 kW and 8 kW.

The grain size of the deposited TiAlN coating decreases as the sputter power increases as reflected in Table 4. The decrease in grain size can be attributed to higher number and greater energy of the depositing atoms onto the substrate surface. This condition is more favourable for the nucleation of new grains than the growth of existing ones (Wuhrer *et al.*, 2004). This reduction in grain size corresponding to the reduction in surface roughness as reflected in Table 4.

TABLE 4  
The quantitative data from the XRD and EDX analysis for TiAlN coating as the sputtering power increases.

Run	Sputtering Power (kW)	I111/I200	Dp (nm)
18	4	*	24.59
19	6	3.65	12.31
15	8	0.78	8.75
* No I200 peak			

### 3.2 Substrate bias

As reflected in Figure 4, as the substrate bias increases from 100.67 to 175 V the coating roughness decreases from 66.4nm to 55nm and as the substrate bias increases from 175V to 249V, the coating roughness increases from 55nm to 67nm. This quadratic behaviour can also be inferred from the ANOVA analysis in Table 4 where the quadratic term of substrate bias is one of the significant terms that influence coating roughness. This finding is aligned with study by Barshilia and Rajam (Barshilia *et al.*, 2004) that indicated as the substrate bias increased from 0V to 200V, the developed coating roughness reduced significantly. The upward trend of coating roughness beyond certain substrate bias level, as indicated in this study, was also reported by Cheng *et al.* (Cheng *et al.*, 2002). This could be due to imperfection of coating surface caused by bombardment of ions with excessively high energy level above certain substrate bias voltage (Hultman *et al.*, 1987).

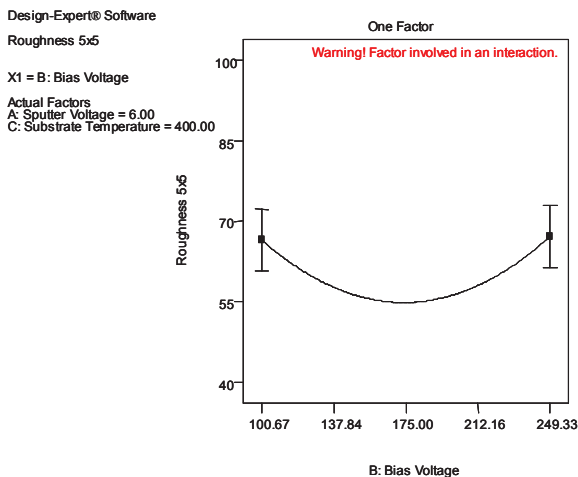


FIGURE 4  
Behavior of coating roughness in response to variation of substrate bias voltage.

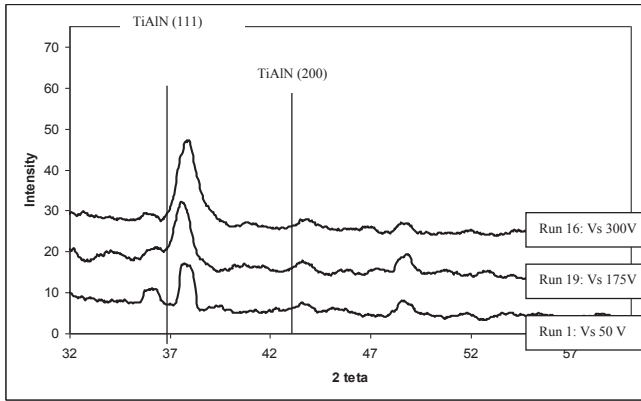


FIGURE 5

$2\theta$  vs. intensity curves for the XRD analysis for substrate bias voltage of 50V, 175V and 300V

The  $2\theta$  vs. intensity curves for the XRD analysis for substrate bias voltage of 50V, 175V and 300V are shown in the Figure 5. Quantitative data from the XRD analysis such as  $I_{111}/I_{200}$  and grain size are tabulated in Table 5.

TABLE 5

TiAlN coating characteristics and microstructure data as substrate bias voltage varies

Run	Bias Voltage (V)	Roughness (nm)	$I_{111}/I_{200}$	$D_p$ (nm)
1	50	81	2.43	59.30
19	175	45	3.65	12.31
16	300	100	3.84	10.66

The intensity ratio data indicates that as the substrate bias increases from 50V to 175V, the  $I_{111}/I_{200}$  increases significantly from 2.429 to 3.654 reflecting shift in crystal orientation from (200) plane towards (111) plane. Subsequent incremental increases in substrate bias from 175 V to 300 V resulted in minimal changes in  $I_{111}/I_{200}$  value. A similar trend in crystal orientation behavior under influence of substrate bias voltage variation was also reported in studies by Matsue *et al.* (2004) and Ahlgren and Blomqvist (2005). Significant grain size reduction was observed from 59.299 nm to 12.309 nm as the voltage increased from 50V to 175 V. Further increase in substrate bias from 175V to 300 V resulted less significant reduction in grain size. The AFM images shown in Figure 6a and 6b provide visual evidence of the reduction of grain size and smoother surface morphology of TiAlN coating as

the substrate bias voltage increases and the respective SEM images of fractured cross section indicate a reduction in porosity and formation of a dense columnar structure at higher bias voltage. The reduction in grain size can be attributed to increases in ion bombardment as a result from substrate bias incremental changes. This is due to higher nucleation density resulting in fine-grained morphology (Barshilia *et al.*, 2004). The energy impacted upon the growing coating, due to ion bombardment, also helps to anneal out imperfections in the coating. However above certain ion bombardment energy level, the damaged induced by ion bombardment is more detrimental than the benefits (Hultman *et al.*, 1987). This is evidence in Figure 6c as the substrate bias was further increased to 300V where imperfection of coating morphology occurred possibly due to resputtering of the deposited coating.

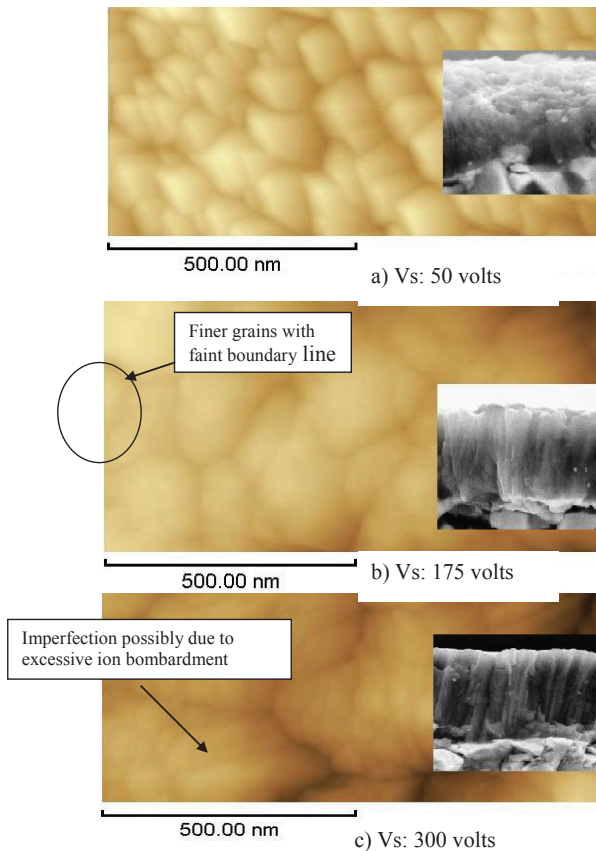


FIGURE 6

AFM image (with imbedded SEM image) indicating the transformation of grain size and morphology of TiAlN coating as the substrate bias increases

### 3.3 Interaction between sputtering power and substrate temperature:

The ANOVA analysis also revealed that one of the significant factors influencing the coating roughness is the interaction between sputtering power and the substrate temperature. As shown in Figure 7, at low substrate temperature level, changes in sputtering power does not significantly affect coating roughness. However at the high levels of substrate temperature, increases in sputtering power significantly reduce coating roughness. This indicates strong interaction exists between these two parameters that affect coating roughness.

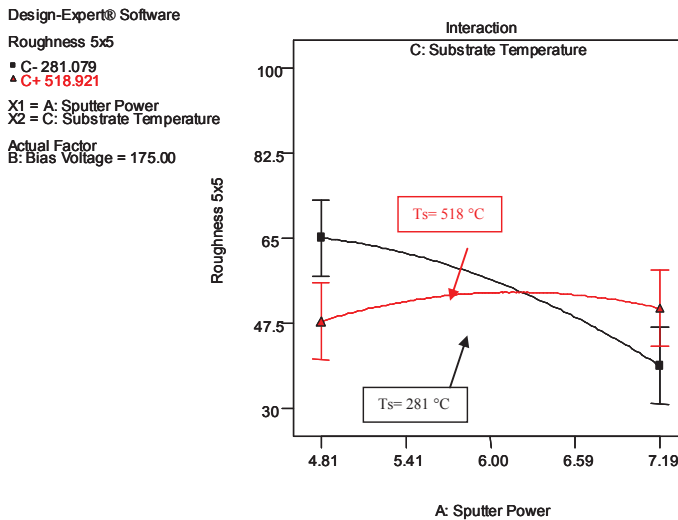


FIGURE 7

Behaviour of coating roughness relative to interaction between sputtering power and substrate temperature.

At high substrate temperature the change in sputtering power has an insignificant effect on the roughness of the TiAlN coating because it suppressed preferential crystal growth which resulted in smoother surfaces (Lugscheider *et al.*, 1996). The lack of preferential growth can be observed in Figure 8 where the peaks of XRD curves for high temperature samples (Run 2 and Run 17) are much less pronounced compared to that of the lower temperature level (Run 11 and Run 6). The AFM images in Figure 9 shows the TiAlN coating morphology, where the coating with high substrate temperature level, Run 2 and Run 17, has a rounded and smoother surface compared to the coating of lower substrate temperature level, Run 6 and Run 11.

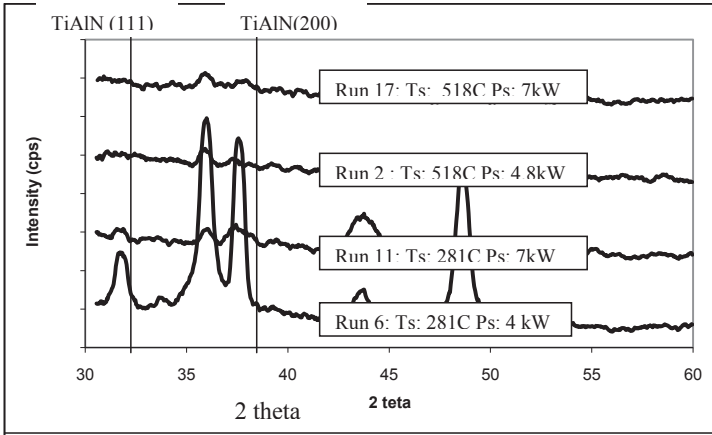


FIGURE 8  
XRD curves to compare the effect of interaction between sputtering power and substrate temperature

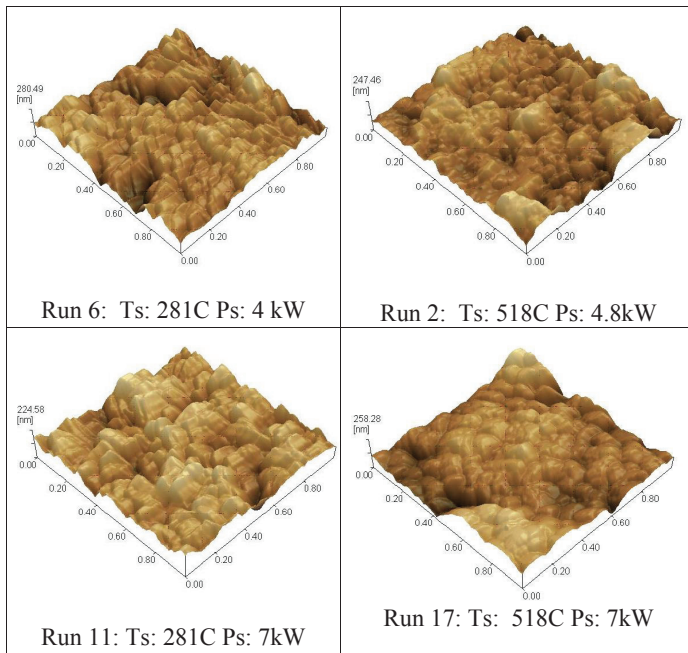


FIGURE 9  
Interaction effect between substrate temperature and sputtering power on the TiAlN coating morphology.

## 4.0 CONCLUSION

TiAlN coatings were deposited using PVD sputtering process at different levels of substrate bias voltages, substrate temperatures, and sputtering powers following the experimental matrix developed based on RSM approach. Findings from this study indicated that sputtering power, interaction between sputtering power and substrate temperature, and substrate bias quadratic term are the significant process parameters that influence the deposited TiAlN coating roughness. Increase in sputtering power resulted in decrease in surface roughness due to finer grain size formation. The Interaction between sputtering power and substrate temperature indicated that at lower substrate temperature level, the change in sputtering power resulted in insignificant change in coating roughness attributed to the suppressed preferential crystal growth which resulted in smoother surfaces. The substrate bias voltage influenced the coating roughness in a quadratic behaviour where increase in substrate bias voltage up to 175V resulted in lower roughness value; however increment beyond that value resulted in higher surface roughness. This was attributed to the resputtering phenomenon which could occur if the ion bombardment energy is excessively high.

## 5.0 REFERENCES

- B. Podgornik,, S. Hogmark, O. Sandberg. 2004. Influence of surface roughness and coating type on the galling properties of coated forming tool steel. *Surface and Coatings Technology* 184. pp 338–348.
- Barshilia Harish C. and Rajam K. S. 2004. Nanoindentation and atomic force microscopy measurements on reactively sputtered TiN coatings. *Bull. Mater. Sci.* 27. pp (1) 35–41.
- Bunshah Rointan F. 1994. *Handbook of deposition technologies for films and coatings*. Second edition. New Jersey. Noyes Publication.
- Byrne G. and Scholta E. 1993. Environmentally clean manufacturing processes/A strategic approach. *Ann. CIRP* 42. pp 471–474.
- Cheng Y. H., Tay B. K. and Lau S. P. 2002. Substrate bias dependence of the structure and internal stress of TiN films deposited by the filtered cathodic vacuum arc. *J. Vac. Sci. Technol. A* 20. pp (4) 1327-1331.
- Cullity B. D. 1972. *Elements of X-ray diffraction*. MA: Addison-Wesley.

- Gekonde Haron O. and Subramanian S. V. (2002) 'Tribology of tool–chip interface and tool wear mechanisms' *Surface and Coatings Technology* 149. pp (2-3) 151-160.
- Hultman L., Helmersson U., Barnett S. A., Sundgren J. E. and Greene J. E. 1987. Low-energy ion irradiation during film growth for reducing defect densities in epitaxial TiN(100) films deposited by reactive-magnetron sputtering. *J. Appl. Phys.* 61. pp 552.
- Laing K., Hampshire J., Teer D., and Chester G. 1999. The effect of ion current density on the adhesion and structure of coatings deposited by magnetron sputter ion plating. *Surf. Coat. Technol.* 112. pp 177–180.
- Lugscheider E. , Barimani C., Wolff C., Guerreiro S., Doepper G. 1996. Comparison of the structure of PVD-thin films deposited with different deposition energies. *Surface and Coatings Technology* 86-87. pp 177-183.
- Mayrhofer Paul H., Mitterer Christian, Hultman Lars, Clemens Helmut. 2006. Microstructural design of hard coatings. *Progress in Materials Science* 51. pp 1032-1114.
- Musil J and Vlcek J. 1998. Magnetron sputtering of films with controlled texture and grain size. *Materials Chemistry and Physics* 54. pp 116-122.
- Smith D.L. 1995. *Thin Film Deposition: Principle & Practice*. New York: McGraw Hill.
- Tuffy K., Byrne G. and Dowling D. 2004. Determination of the optimum TiN coating thickness on WC inserts for machining carbon steels. *Journal of Materials Processing Technology* 155-156. pp 1861-1866.
- Wuhrer R. and Yeung W. Y. 2004. Grain refinement with increasing magnetron discharge power in sputter deposition of nanostructured titanium aluminium nitride coatings. *Scripta Materialia* 50, pp. 813–818.
- Xu Xuan-qian, Ye Hui, Zou Tong. 2006. Characterization of DC magnetron sputtering deposited thin films of TiN for SBN/MgO/TiN/Si structural waveguide. *J Zhejiang Univ SCIENCE A* 7. pp (3) 472-476.